COBEM 2023
27TH INTERNATIONAL CONGRESS OF MECHANICAL ENGENEERING

ABCM
Brazilian Society of Mechanical Sciences and Engineering
27th ABCM International Congress of Mechanical Engineering
December 04-08, 2023, Florianópolis-SC, Brazil

COB-2023-0068
DYNAMIC ANALYSES (MODAL AND FORCE VIBRATION) IN A RAILWAY VEHICLE MODEL WITH 25 DEGREES OF FREEDOM

Fernando Luiz Martinechen Beghetto
Federal University of Technology – Paraná.
Rua Deputado Heitor Alencar Furtado, 5000 - Ecoville.
CEP 81280-340 - Curitiba – PR – Brazil.
e-mail flbeghetto@utfpr.edu.br

Abstract. *In this work, the modal and the forced vibration dynamic analyses are carried out in a railway vehicle model with 25 degrees of freedom. The objective of this work is to study the dynamic characteristics (modes and frequencies of vehicle vibration), as well as the analysis of forced vibration, allowing the simulation of resonance conditions and their critical speeds, important for the study of vehicle stability, safety and passengers comfort. The tridimensional model has a passenger car body, two bogies and four wheelsets. Models of vertical, lateral and rotational track irregularities are used. In mechanical contact between wheels and rails, the theories of Hertz and Kalker, and also Vermeulen and Johnson are used. The equations of motion of the coupled system are numerically integrated using the Newmark method, in the MatLab software. It is possible to conclude that the railway track irregularities associated with critical traffic speeds produce vibrations in the vehicle. Due to the damping of the system, these vibrations are attenuated between the rigid bodies through the primary suspensions, between the wheels and bogies; and secondary suspensions, between the bogies and the passenger car body.*

Keywords: *Railway Vehicle, Track Irregularities, Mechanical Contact.*

1. INTRODUCTION

The railway transport in Brazil stand out for the number of passengers to be transported, when compared to other transports types. In Rio de Janeiro's SuperVia, more than 1 million passengers are transported daily. In São Paulo's CPTM, more than 5.3 million passengers are transported daily. This modal is also used in others Brazilian cities: Fortaleza (CE), Natal (RN), João Pessoa (PB), Recife (PE), Maceió (AL), Salvador (BA), Brasília (DF), Belo Horizonte (MG) and Porto Alegre (RS).

The objective of this work is to carry out a modal dynamic analysis and forced vibration in a railway vehicle through computational models, considering track irregularities and mechanical contact between wheels and rails.

2. RAILWAY VEHICLE MODEL

The Figure 1 illustrates the model with its respective 25 degrees of freedom.

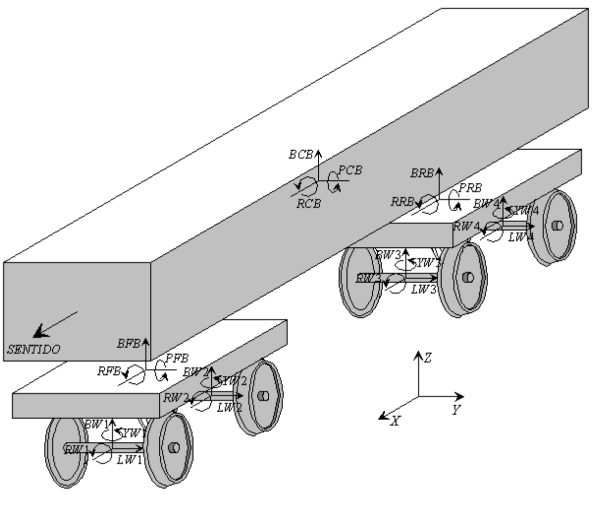

Figure 1. Railway vehicle model.

The present model is conceived through the association of rigid bodies interconnected to suspensions systems. It has four wheelsets interconnected to the two bogies through the primary suspensions. The bogies in turn are interconnected to the car body by the secondary suspensions. The equations of motion are obtained through dynamic equilibrium. This model is capable of representing 25 degrees of freedom of motion, namely: bouncing, rolling and pitching of the car body, bouncing, rolling and pitching of the bogies, and bouncing, lateral, rolling and yawing of four wheelsets. These equations of motion can be written as matrix system of second order differential equations below:

$$[M_V]\{\ddot{U}_V(t)\}+[C_V]\{\dot{U}_V(t)\}+[K_V]\{U_V(t)\}=\{P_V(t)\}. \tag{1}$$

Where $[M_V]$, $[C_V]$, and $[K_V]$ are the mass, damping, and stiffness matrices, respectively, and $\{\ddot{U}_V(t)\}$, $\{\dot{U}_V(t)\}$, $\{U_V(t)\}$, and $\{P_V(t)\}$ are the acceleration, velocity, displacement and external forces vectors, respectively. The complete formulation and its respective developments are presented in detail in (Beghetto, 2011).

The dynamic properties of the vehicle, and the geometric distances are shown in Tables 1 and 2, respectively.

Table 1. Dynamic properties of the vehicle.

Vehicle Parts	**Parameters**	**Values**	**Units**
Car body	Mass	49,120	kg
	Mass moment of inertia (rolling)	64,050	kg.m²
	Mass moment of inertia (pitching)	2008,950	kg.m²
Front bogie	Mass	11,000	kg
	Mass moment of inertia (rolling)	8,750	kg.m²
	Mass moment of inertia (pitching)	20,800	kg.m²
Rear bogie	Mass	11,000	kg
	Mass moment of inertia (rolling)	8,750	kg.m²
	Mass moment of inertia (pitching)	20,800	kg.m²
Wheelsets	Mass	1,500	kg
	Mass moment of inertia (rolling)	989	kg.m²
	Mass moment of inertia (yawing)	989	kg.m²
Primary suspension	Spring coefficient	1637,275	N/m
	Damping coefficient	32,7455	N.s/m
Secondary suspension	Spring coefficient	875,655	N/m
	Damping coefficient	17,5131	N.s/m
Lateral links	Spring coefficient	100,000	N/m
	Damping coefficient	2,000	N.s/m
Longitudinal links	Spring coefficient	100,000	N/m
	Damping coefficient	2,000	N.s/m

Table 2. Geometric distances.

Distances	**Values**	**Units**
Longitudinal distance of centre of bogies	15	m
Longitudinal distance of centre of wheelsets	2.6	m
Cross distance of centre of wheelsets	2.5	m

3. TRACK IRREGULARITIES MODELS

The wheelsets vibration are produced by track irregularities through the mechanical contact between wheels and rails profiles. The wheelsets motion's are absorbed by the primary suspensions, and transmitted to the bogies. These transmit the damped vibrations to car body throught secondary suspensions.

The length of the railtrack in this simulation is 300m, and various track irregularities models combinations are used to produces vibrations. The vertical model is based on sinusoidal harmonic functions, (Dahlberg, 2006). The amplitudes used are 10mm, and the lengths are varied to (1m, 2m, 2.5m, 7.5m and 10m), allowing to simulate the amplification of the dynamic responses of the vehicle.

For new profiles of wheelset and rails, the variation of the gauge are assumed (9mm to 15mm), in according to (Brina, 1979). The lateral model of track irregularities is also based on sinusoidal harmonic functions. The hunting motion of the wheelsets through the track is composed of a translation and rotation simultaneously, modeled by the cosinusoidal harmonic functions with 18.234m of wavelength, (Pombo et al., 2009).

4. WHEEL-RAIL CONTACT MODELS

In according to Hertz's theory, when compressing two elastic bodies with curved surfaces, due to the mutual deformation of these bodies, the contact area generated will be an ellipse, (Timoshenko and Goodier, 1980).

In (Kalker, 1990), contact with a certain amount of slippage between surfaces is considered, which is limited by the Vermeulen and Johnson's model, (Iwnicki, 2003), (Pombo et al., 2009). In this model, the tangential contact force and the spin rotation moment are restricted to a cubic polynomial. Contemplating the geometric nonlinearities due to the profiles of the wheels and the rails, and the limits of adhesion in the contact between these bodies.

5. MODAL ANALYSES OF THE VEHICLE

Widely used for the characterization of dynamic systems, modal analysis determines the circular natural frequencies (eigenvalues) and their respective vibration modes (eigenvectors). One can find ways to solve the problem in question in (Chopra, 1995), and (Bathe, 1996).

The Table 3 presents the circular natural frequencies (ω_n), the damped circular natural frequencies (ω_d), the cyclic natural frequencies (f_n), the damped cyclic natural frequencies (f_d), the periods of natural vibration (T_n), the periods of damped natural vibration (T_d), and the damping ratios (ζ_v) of the vehicle. The type of damping is classic.

Table 3. Frequencies, periods and damping ratios.

Nº	**ω_n (rad/s)**	**ω_d (rad/s)**	**f_n (Hz)**	**f_d (Hz)**	**T_n (s)**	**T_d (s)**	**ζ_v**
1st	8,165	8,138	1,300	1,295	0,770	0,772	0,082
2nd	13,923	13,787	2,216	2,194	0,451	0,456	0,139
3rd	14,84	14,676	2,362	2,336	0,423	0,428	0,148
4th	15,896	15,694	2,530	2,498	0,395	0,400	0,159
5th	17,776	17,493	2,829	2,784	0,353	0,359	0,178
6th	18,365	18,053	2,923	2,873	0,342	0,348	0,184
7th	52,107	44,474	8,293	7,078	0,121	0,141	0,521
8th	53,057	44,975	8,444	7,158	0,118	0,140	0,531
9th	71,926	49,97	11,447	7,953	0,087	0,126	0,719
10th	80,018	47,991	12,735	7,638	0,079	0,131	0,800

Here, only the first ten modes and frequencies are used, as the upper ones represent only rigid body motion. The natural, normalized modes of vibration are presented in the forced vibration analyses under the system's resonance conditions.

6. FORCED VIBRATION ANALYSES OF THE VEHICLE

The forced vibration of the vehicle will have as an external excitation source, track irregularities, associated with traffic speed. The equations of motion are integrated using the Newmark Method, with average acceleration, (Bathe, 1996). The system of linear equations is solved using the Gauss Elimination Method, (Burden and Faires, 2003).

Resonance will occur when the external excitation coincides with the damped circular natural frequencies (ω_d). The vehicle will offer the resonant speeds (V_R) which are obtained through the damped circular natural frequencies (ω_d) and the lengths of the irregularities (l_I), as follows:

$$\omega_d = \omega_I ; \omega_I = 2.\pi.f_I = \frac{2.\pi.V_R}{l_I} ; V_R = \frac{\omega_d . l_I}{2.\pi} . \tag{2}$$

Under the resonance condition, there will be amplification of the dynamic, displacement (R_D), velocity (R_V), and acceleration (R_A) responses, which can be written as follows:

$$R_D = R_A = \frac{1}{2.\xi_v.\sqrt{1-\xi_v^2}} ; R_V = \frac{1}{2.\xi_v} . \tag{3}$$

With the values of the damping ratios listed in Table 3, the dynamic amplification factors for the displacement, velocity and acceleration responses in the vehicle's vibration modes are determined. The critical speeds of the vehicle in resonance condition, and respective dynamic amplification factors are presented in Table 4. It is possible to observe that at low frequencies, greater amplification occurs, since the damping ratio is lower in these situations.

Table 4. Critical speeds, and dynamic amplification factors of the vehicle.

Modes	**1st**	**2nd**	**3rd**	**4th**	**5th**	**6th**	**7th**	**8th**	**9th**	**10th**
V_R (km/h)	85	59	84	67	30	78	25	64	57	55
$R_D = R_A$	6.118	3.632	3.416	3.185	2.855	2.765	1.124	1.111	1.001	1.042
R_V	6.098	3.597	3.378	3.145	2.809	2.717	0.960	0.942	0.695	0.625

In Figure 2, it is observed that the 1st vibration mode is responsible for the lateral vibration of the wheelsets.

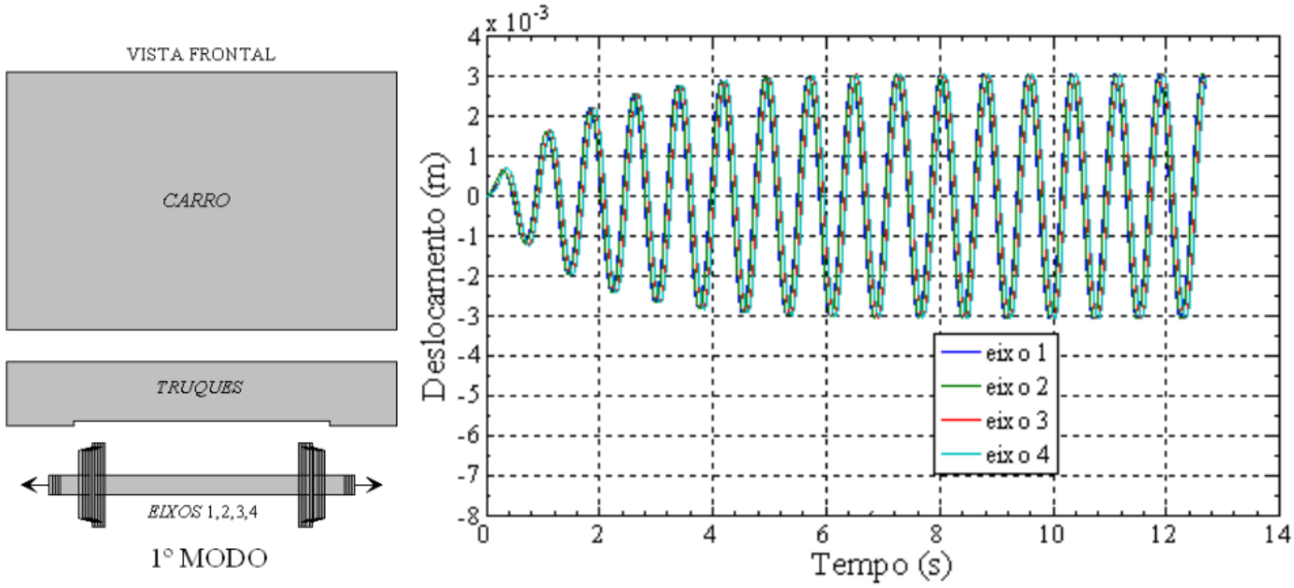

Figure 2. Forced vibration in 1st mode.

The transient dynamic response illustrates the harmonic oscillatory behavior, according to the irregularities model used. The behavior of the wheelsets is similar. The maximum displacement amplitudes are of the order of 3mm, proving to be relatively low in this presented simulation.

In Figure 3, it is observed that the 2nd mode of vibration is responsible for the vertical vibrations of the car body, the front and rear bogies, and the wheelsets.

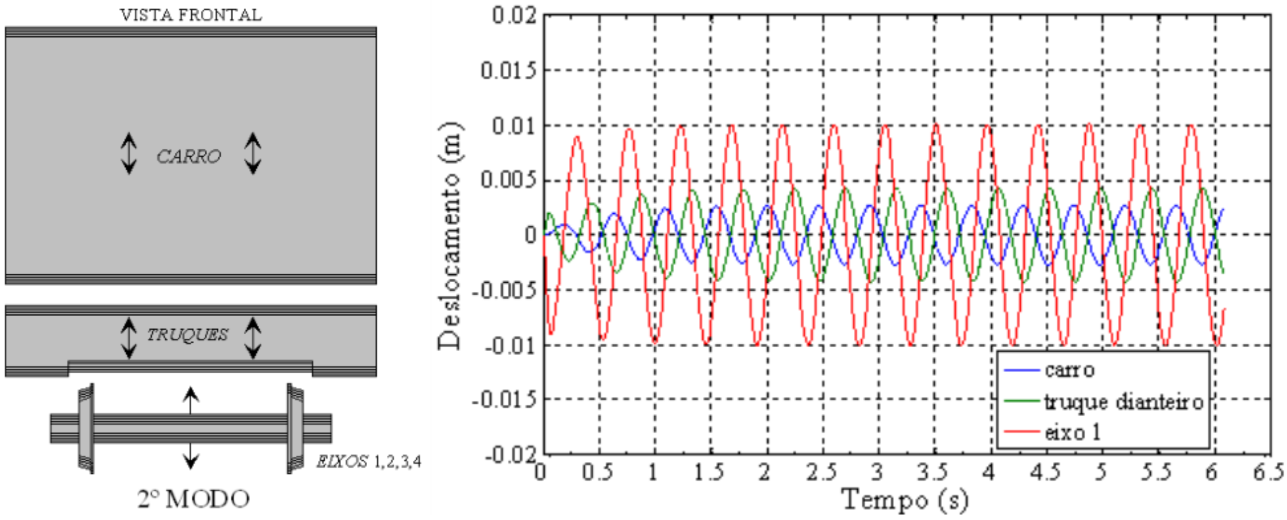

Figure 3. Forced vibration in 2nd mode.

The vibration behavior of the wheelsets are similar to each other, therefore, only the vibration of wheelset 1 was presented here. The same occurs between the front and rear bogies, therefore, only the vibration of the front bogie is presented here. It is noticed that the amplitudes of displacement of wheelset 1 are greater than those presented by the bogies, due to the presence of the primary suspensions. Those of the car body are smaller than those of the bogies, attenuated due to the secondary suspensions. Despite the resonant condition, the displacements are out of phase, due to the different geometry of the rigid bodies, under the irregularity model used. The displacement amplitudes presented are relatively small.

In Figure 4, it is observed that the 3rd mode of vibration is responsible for the vertical vibrations of the wheelsets, of the front and rear bogies, and the rotation movement (pitching) of the car body.

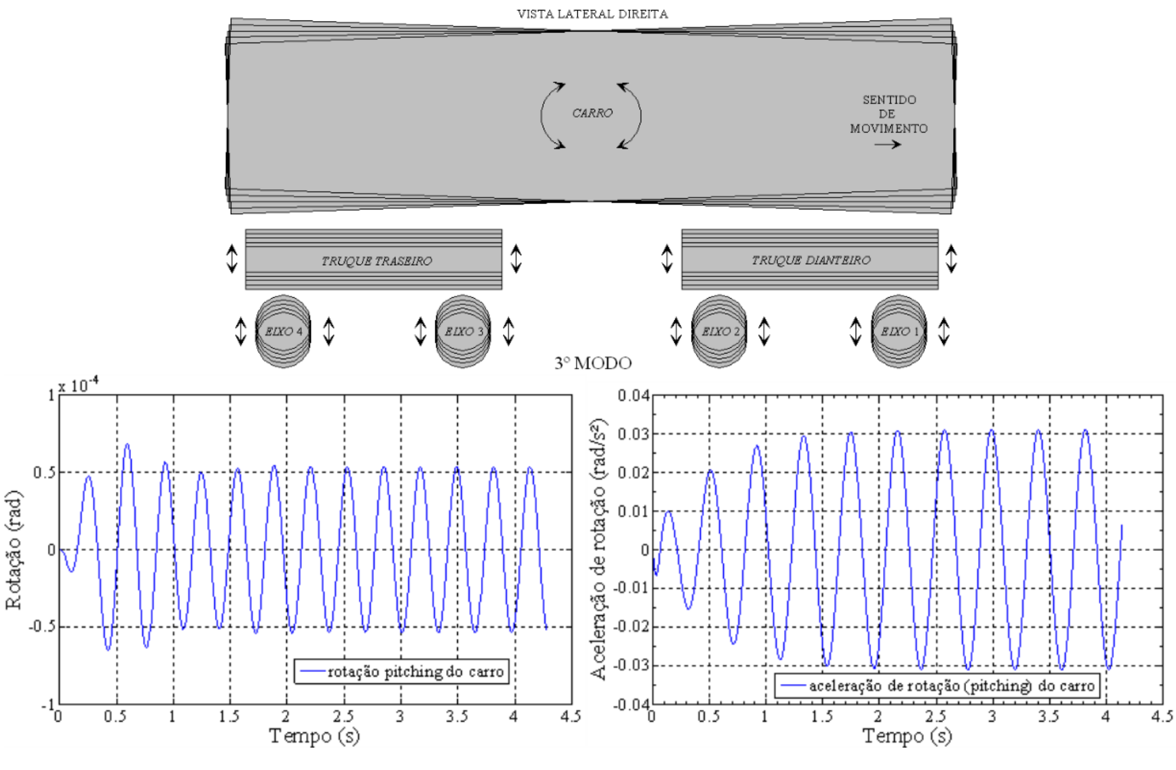

Figure 4. Forced vibration in 3rd mode.

To induce the latter, without phase cancellation in the front and rear bogies, as well as in the wheelsets, a wavelength of 10m and amplitude of 10mm was used in the irregularities model.

Note an oscillatory movement according to the irregularity model used. The amplitudes of rotation (pitching) of the car body, as well as the produced angular accelerations are relatively small, for the simulation carried out.

In Figure 5, it is observed that the 4th mode of vibration is responsible for the rotational vibrations (rolling) of the front and rear bogies, and of the wheelsets. In this simulation, in the model of vertical irregularities used, the combination of lag between the amplitudes of the right and left rails was made, allowing, in this way, to analyze the behavior of this mode of vibration. There is an amplification in the dynamic response of the front bogie, in relation to the rear bogie. The same occurs between wheelsets 1 and 2, belonging to the front bogie, when compared to wheelsets 3 and 4, belonging to the rear bogie. In the car body, the response is attenuated, in relation to the bogies.

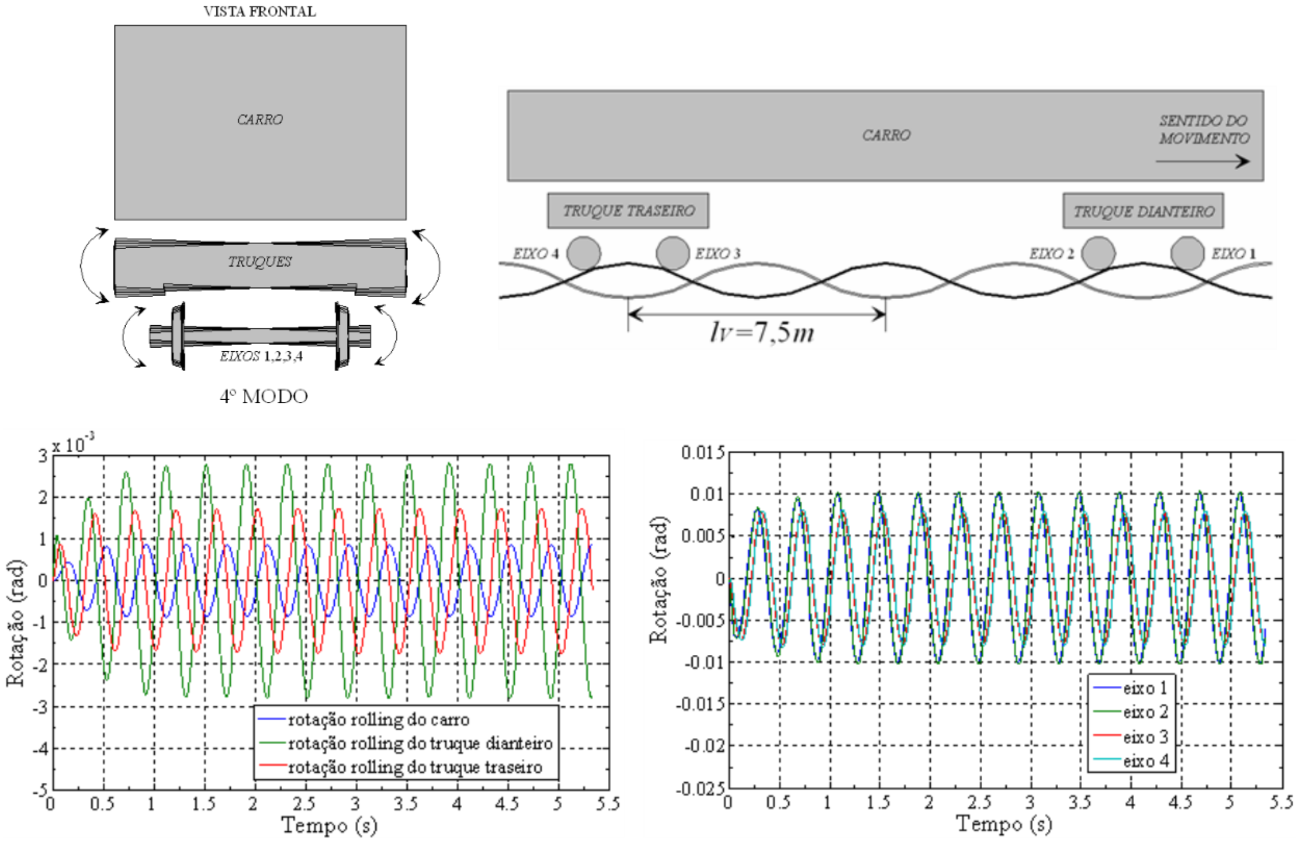

Figure 5. Forced vibration in 4th mode.

In Figure 6, it is observed that the 5th mode of vibration is responsible for the rotational vibrations (yawing) of the wheelsets. To induce this hunting behavior in the wheelsets, we used the calculation of the wavelength at which the phenomenon occurs, which was studied by Klingel and Boedecker, (Pombo et al., 2007), and results in 18.234m, associated with the adopted rotational irregularities model. According to the studies by (Mohan, 2003), this phenomenon occurs in conditions of relatively low speed, in this case, for the excitation of the present mode, according to Table 4, there is the condition of critical speed (resonant) of 30km/h. The amplitudes found are relatively small.

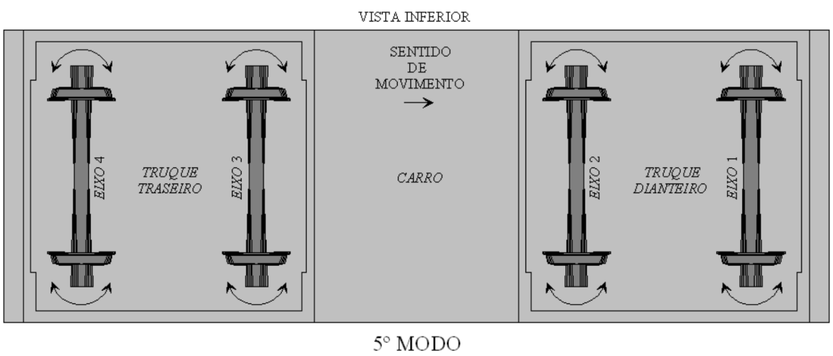

Figure 6. Forced vibration in 5th mode.

In Figure 7, it is observed that the 6th mode of vibration is responsible for the vibrations of rotation (rolling) of the car body, the front and rear bogies, and the wheelsets. The vibration amplitudes of the front bogie are greater than those presented by the rear bogie, and they present a phase shift. Again the vibrations of the car body are less than those presented by the bogies. The angular acceleration is relatively small.

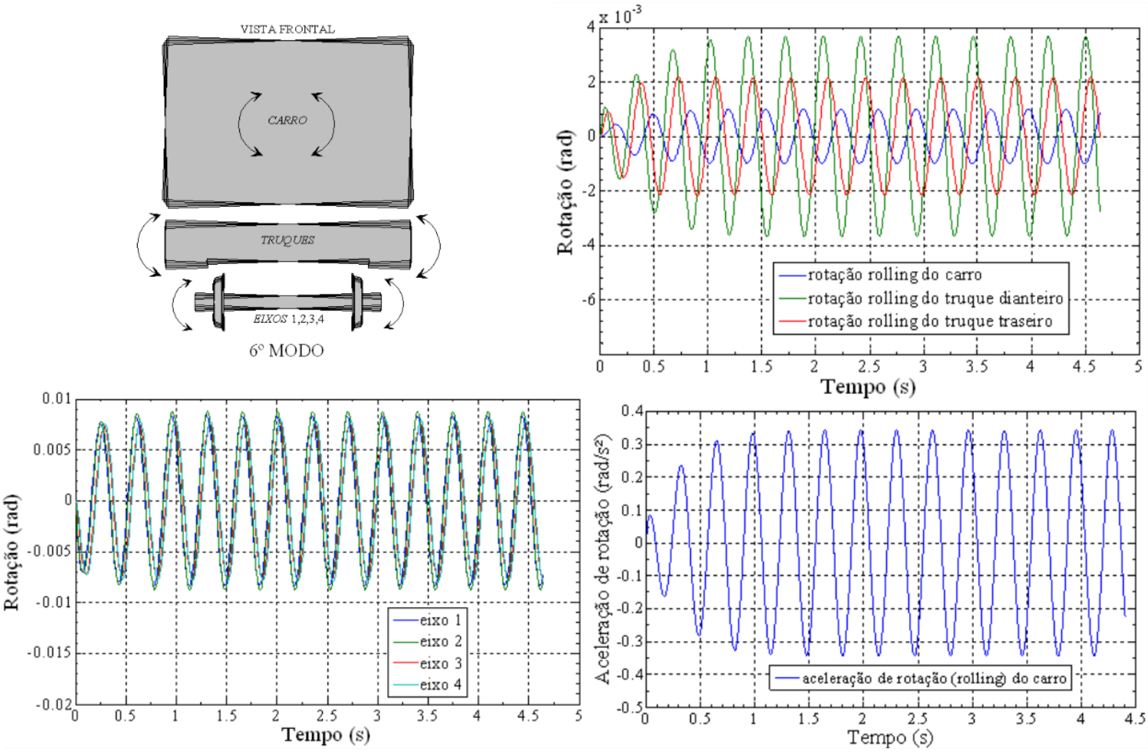

Figure 7. Forced vibration in 6th mode.

In Figure 8, it is observed that the 7th mode of vibration.

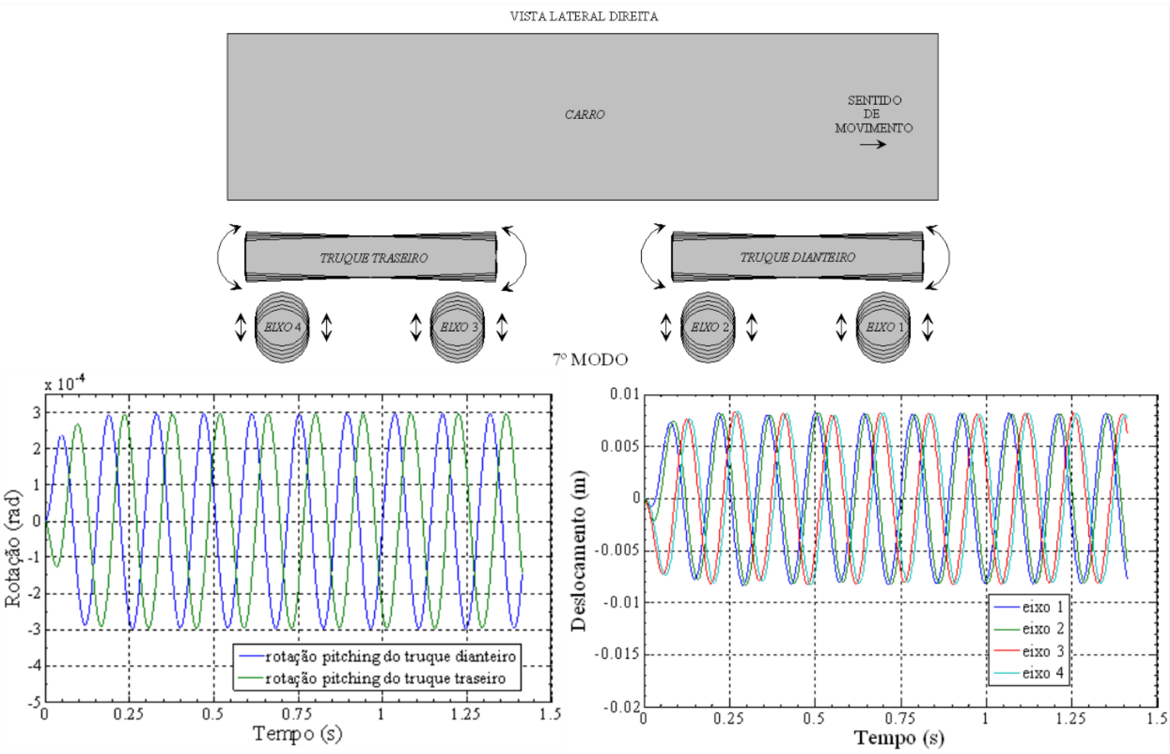

Figure 8. Forced vibration in 7th mode.

This vibration mode is responsible for the vertical vibrations of the wheelsets, and rotations (pitching) of the front and rear bogies. In this simulation, amplitudes of 10mm and lengths of 1m were used in the model of vertical irregularities to induce the amplification of the rotation (pitching) of the front and rear bogies. There is a similar behavior between the wheelsets, presenting the same amplitudes, however lagged. The vertical displacements of the wheelsets are given in pairs, according to the front and rear bogies, respectively. Small displacement amplitudes are presented.

The relevance of choosing the wavelength of the vertical track irregularities model was noticed throughout the simulations, as it can lead to signal amplification or attenuation due to phase cancellation. It is noteworthy that the choice of wavelength will influence the critical (resonant) speed, according to Eq. (2) presented.

7. CONCLUSIONS

In this work it was possible to analyze the dynamic behavior of a railway vehicle, in free vibration and in forced vibration produced by track irregularities associated with operating speeds.

In the free vibration analysis, the frequencies and respective modes of vibration of the system were obtained, which presented classical damping. The damping ratios shown increase for higher natural frequencies. Vibration modes excite different vehicle degrees of freedom. The higher modes present only rigid body motion, and were neglected in the study. In the forced vibration analysis, models of vertical, lateral and rotational irregularities were used, combined with each other, allowing the simulation of the most unfavorable vibration conditions. The critical (resonant) speeds of the vehicle in unfavorable situations were determined.

In general, the dynamic responses presented are consistent with the track irregularities models used, presenting a harmonic and periodic behavior. The amplitudes of the dynamic responses presented in the proposed simulations were relatively small. The influence of the primary and secondary suspension systems was noticed, significantly reducing the dynamic responses of the bogies, and mainly of the car body.

8. REFERENCES

Bathe, K. J., 1996. Finite Element Procedures. Prentice-Hall, New Jersey.

Beghetto, F. L. M., 2011. Modelagem tridimensional da interação dinâmica entre veículo e ponte ferroviária considerando contato roda-trilho, irregularidades da via e variação de velocidade. Tese (Doutorado), Pontifícia Universidade Católica do Paraná, Curitiba.

Brina, H. L., 1979. Estradas de Ferro. Volume 1. Via Permanente. Livros Técnicos e Científicos Editora.

Burden, R. L., Faires, J. D., 2003. Análise Numérica, Ed. Thomson.

Chopra, A. K., 1995. Dynamics of Structures: Theory and applications to earthquake engineering. Prentice-Hall, New York.

Dahlberg, T., 2006. Handbook of Railway Vehicle Dynamics, Track Issues, Taylor & Francis Group, LLC.

Iwnicki, S., 2003. Simulation of wheel-rail contact forces. *Fatigue Fracture Engineering Materials Structures*, n. 26, p. 887-900.

Kalker, J. J., 1990. Rolling contact phenomena: Linear Elasticity. Delft University of technology.

Mohan, A., 2003. Nonlinear investigation of the use of controllable primary suspensions to improve hunting in railway vehicles. Master of Science in Mechanical Engineering Thesis, Faculty of Virginia Polytechnic Institute and State University, Blacksburg, Virginia, USA.

Pombo, J. et al., 2007. A new wheel-rail contact model for railway dynamics. IDMEC– Instituto Superior Técnico, Lisboa, Portugal.

Pombo, J. et al., 2009. Wheel wear evolution and its influence on the dynamic behaviour of railway vehicles. *7th EUROMECH Solid Mechanics Conference*, Lisbon, Portugal, September 7-11.

Timoshenko, S. P., Goodier, J. N., 1980. Teoria da Elasticidade. 3º Edição, McGraw-Hill, Editora Guanabara Koogan, S.A.

9. RESPONSIBILITY NOTICE

The author is the only responsible for the printed material included in this paper.